



**HAL**  
open science

## Short-pulse laser-produced plasmas

Jean-Claude Gauthier

► **To cite this version:**

Jean-Claude Gauthier. Short-pulse laser-produced plasmas. Yamanouchi, K.; Chin, S.L.; Agostini, P.; Ferrante, G. Progress in Ultrafast Intense Laser Science I, Springer Series in Chemical Physics, springer, pp.122, 2006. hal-00224829

**HAL Id: hal-00224829**

**<https://hal.science/hal-00224829v1>**

Submitted on 30 Jan 2008

**HAL** is a multi-disciplinary open access archive for the deposit and dissemination of scientific research documents, whether they are published or not. The documents may come from teaching and research institutions in France or abroad, or from public or private research centers.

L'archive ouverte pluridisciplinaire **HAL**, est destinée au dépôt et à la diffusion de documents scientifiques de niveau recherche, publiés ou non, émanant des établissements d'enseignement et de recherche français ou étrangers, des laboratoires publics ou privés.

# Short-Pulse Laser-Produced Plasmas

Jean-Claude Gauthier

Centre Lasers Intenses et Applications (CELIA)  
UMR 5107 CNRS, CEA, Université Bordeaux 1, 33405 Talence (France)  
gauthier@celia.u-bordeaux1.fr

**Summary.** In this review, the physics of short-pulse laser-produced plasmas at moderate intensities is described, together with applications to x-ray sources and material processing.

## 1 Introduction

In the 80s, advances in laser science and optical technologies have opened new possibilities in the study of laser-produced plasmas. One of these advances is the implementation of the Chirped Pulse Amplification (CPA) technique [1] which has created new opportunities in the domain of ultra-intense and ultrafast laser physics. The interactions of ultra high-intensity laser pulses with matter have opened the field of optics in relativistic plasmas, a new topic of high-field science presented in comprehensive reviews [2, 3]. Indeed, intense lasers have been used to accelerate beams of electrons [4] and protons [5] to energies of several megaelectronvolts in distances of only microns. Recent improvements in particle energy spread [6] may allow compact laser-based radiation sources to be useful someday for cancer hadrontherapy [7] and as injectors into conventional accelerators [8], which are critical tools for x-ray and nuclear physics research. They might also be used for “fast ignition” [9] of inertial fusion targets. The ultrashort pulse duration of these particle bursts and the x rays they can produce, hold great promise as well to resolve chemical, biological or physical reactions on ultrafast time scales and on the spatial scale of atoms [10]. Indeed, the time duration of these pulses being less than 100-fs, this is shorter than the time-scale of significant hydrodynamic motion of ions or solid target surfaces. Consequently, solid-density matter may be heated from room temperature to several hundreds of electronvolts without the usual change in density that accompanies long-pulse irradiation [11]. Ultrafast plasmas have important applications in material processing [12], thin film growth using ultrafast pulsed-laser deposition [13], and ultrashort pulse x-ray sources [14].

In this short review, we concentrate on “low” (non-relativistic) laser intensities, i.e.  $I\lambda^2$  below a few  $10^{18}$   $\text{Wcm}^{-2}\mu\text{m}^2$ , where  $I$  and  $\lambda$  are the laser intensity and wavelength, respectively. We give credit to pioneering

experimental works with femtosecond lasers aimed at producing dense plasmas in Sect.2. In Sect.3 we describe optical techniques to study ultra-short pulse plasma phenomena, including pump-probe techniques and Frequency-Domain Interferometry (FDI), a very powerful optical technique with many applications in ultrafast science. Sect.4 presents the most significant results in x-ray spectroscopy of ultrafast plasmas and describes recent advances in x-ray sources from short-pulse laser-produced plasmas. Sect.5 reviews ultrafast plasma modeling and Sect.6 details some practical applications of femtosecond laser-matter interaction.

## 2 Pioneering works on ultrafast plasmas

In the “long” (nanosecond) pulse regime, laser-plasma interaction physics has been studied extensively to explore the efficiency of collisional absorption by inverse bremsstrahlung, parametric instability growth rates [15], filamentation, x-ray conversion efficiency and hydrodynamic instabilities [16]. In the short pulse regime of laser interaction with solid targets, a key issue is the understanding of the initial processes leading to the production of hot dense plasmas [17,18]. It is crucial to obtain a time- and space-resolved picture of the very steep gradient around the critical density region to study the laser absorption mechanisms. Indeed, most of the energy transfer between the laser and the solid target occurs [19–21] in plasma regions where  $0.5n_c < n_e < 10n_c$  where  $n_c$  is the critical density. With lasers of  $\approx 100$ -fs duration, hydrodynamic simulations (see Sect.5) show that the gradient scale length  $L$  can be very much smaller than the laser wavelength  $\lambda$  and that typical expansion velocities are in the 0.1-nm/fs range. Absorption occurs within

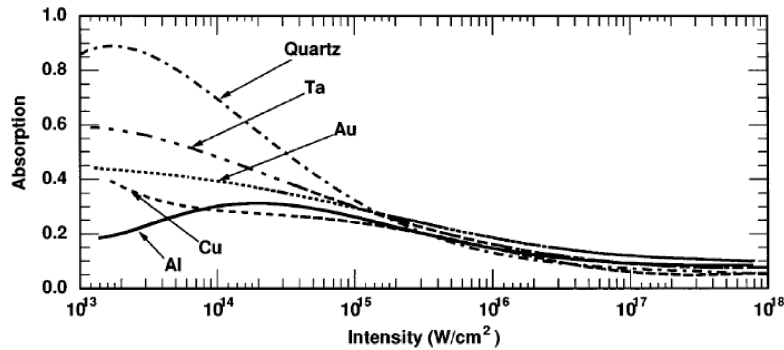


**Fig. 1.** Absorption coefficient of a  $\approx 100$ -fs duration laser in different materials as a function of intensity. (From Ref. [22])

a layer thickness of a skin depth ( $\approx 10$ -nm) [23–26]. At normal incidence in the

Fresnel limit ( $\lambda \ll L$ ) and a metallic target, laser absorption is quite small and the coupling of laser energy to target electrons is very inefficient (see Fig.1). In the WKB limit ( $\lambda \geq L$ ), absorption can be calculated simply [15] using “long” laser pulse formulas and in P-polarization, a peculiar absorption mechanism dubbed “resonance absorption” occur when the component of the laser field perpendicular to the target surface drives electron plasma waves at or below critical density (depending on the incidence angle). In the intermediate regime, numerical solutions of the Helmholtz equations must be derived. The basics of laser absorption mechanisms have been described in detail in Ref. [11].

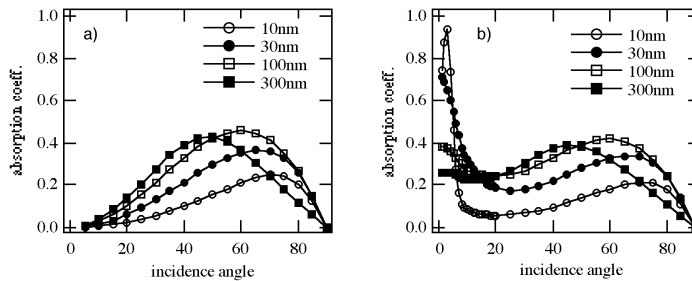
Driven by x-ray sources applications and to circumvent the low absorption registered in the short pulse regime [27, 28], there had been a great deal of interest in methods that could enhance the x-ray yield. The influence of various laser and target conditions has been the subject of many recent studies. Preplasma formation has been investigated in detail as one of the prominent ways of improving the x-ray yields [29]. While significant enhancement in the emission is noticed, it has also been shown that the x-ray pulse duration tends to become longer in such cases [30, 31]. The role of modulation/roughness of the surface in increasing the coupling of the input light into the plasma, which results in an enhancement in the x-ray yield, has been studied in detail. Several authors [32, 33] have shown laser light absorption of over 90% into the plasma formed on grating targets as well as those coated with metal clusters. More recently, impressive enhancements of x-ray flux have been achieved in nanohole alumina, porous silicon targets [34] and nickel velvet targets [35].

Figure 2 shows the absorption coefficient as a function of the incidence angle for different plasma scale length  $L$  calculated with a model of laser-plasma interaction with a grating target [33]. We find a good qualitative agreement, both in incidence angle position and absorption fraction (see Fig.2a), between the crude model and more involved calculations [20, 21] with a flat target. In particular, the fact that the absorption maximum is displaced towards grazing angles for steep electron density gradients is in accord with more elaborate calculations of resonance absorption [15]. In Fig.2b, we have plotted the absorption coefficient calculated for a 100-nm depth grating. The groove spacing  $d$  of the grating has to be correctly chosen to realize the “phase matching” condition ( $k_g = 2\pi/d$ ;  $k_y = k_g + k_0 \cos\theta$ ) where  $k_0$  and  $k_y$  are the radiation wavevectors in vacuum and perpendicular to the grooves, respectively. A sharp peak is observed close to the resonance angle for the 10-nm gradient scale length. A larger absorption is observed below  $20^\circ$  in the case of the grating compared to the case of the flat target. This can be easily explained because, even near normal incidence, there is always a component of the incident electric field parallel to the local electron density gradient. Efficient x-ray production above 1-keV using femtosecond has been demonstrated [36] with laser-produced plasmas on silicon gratings of 1600-nm period and 250-nm groove depth. For long pulse irradiations (1.5-ps), the spectral shape of

shifted- $K\alpha$  transitions is similar to the one obtained previously [37] with flat targets. For short pulses (120-fs) and good laser intensity contrast ( $10^{-6}$ ), the spectral width of these transitions is surprisingly large, indicating electron densities well in excess of  $10^{23} \text{ cm}^{-3}$ . Two-dimensional particle-in-cell simulations indicate that the grating corrugation shape remains imprinted in the plasma during several tens of femtoseconds, increasing the period of time during which laser absorption is resonantly enhanced and favoring radiation emission at high electron densities.

### 3 Optical characterization and pump-probe techniques

Different techniques have been used to study the early evolution of ultra-fast plasmas on a picosecond or subpicosecond time scale. Most of them rely on pump/probe techniques in which a short duration probe pulse interrogates the plasma surface at different time delays after the pump, plasma-producing, pulse. For example, subpicosecond time-resolved Schlieren measurements have been used to locate the critical density layer of a plasma [38]. However, diffraction effects limit the spatial resolution along the target normal to a value of the order of a few laser wavelengths. Analysis of the spectrum of the specular backscattered laser have been used to monitor the critical surface expansion [39–41]. Similar experiments have been performed in gases [42–44] and clusters [45]. A more efficient method to probe the plasma expansion relies on the spectral analysis of a reflected auxiliary beam at different delays. In some experiments, [46–48] expansion velocities have been inferred from Doppler shifts. However, the large spectral width  $\Delta\omega \times \Delta t \approx 2\pi$  of Fourier-transform-limited short pulses makes it difficult to estimate frequency shifts much less than  $\Delta\omega$ . The measurement of the plasma reflectivity difference for S- and P-polarized light as a function of the angle of incidence has also been used to extract information on the gradient scale length [49]. All



**Fig. 2.** Calculated absorption fraction as a function of the angle of incidence on a) flat target and b) grating, as a function of the gradient scale length in nm.  $\lambda=1000\text{-nm}$ , groove spacing  $890\text{-nm}$ , groove depth  $100\text{-nm}$ .

these methods rely on intensity or spectroscopic measurements which are very sensitive to the detrimental shot-to-shot frequency and spatial fluctuations of the lasers.

Optical methods giving access to the phase shift of a probe beam in transmission or reflection have shown their usefulness in the study of surfaces, interfaces, and thin films [50]. In the realm of laser-produced plasmas, Frequency-Domain Interferometry (FDI) is a new technique [51] that enables to measure both the amplitude and the phase of the complex reflection coefficient of a plasma with simultaneously high spatial and temporal resolution. In recent years, this technique has been used in ultrafast laser-matter interaction experiments including molecular spectroscopy [52], laser-induced dielectric damage [53, 54], laser wakefield particle acceleration [55], and the study of the propagation and breakout of femtosecond shock waves [56–58]. In laboratory plasmas, this technique has been successfully exploited to measure the electron density gradient scale-length [59], the onset of optical breakdown in dielectric materials [60], the collisionality of ultrafast plasmas [61], and its applicability has been extended to single-shot measurements [62, 63]. FDI has also been used at short wavelengths to probe plasmas with high order harmonic generation in gases [64].

To summarize, FDI probes the plasma surface with two successive twin femtosecond pulses separated in time by an external Michelson interferometer. The power spectrum of a double pulse sequence presents a fringe pattern with an envelope which is the Fourier transform of the pulse duration, modulated with a period inversely proportional to the pulse separation. Any phase shift due to the plasma generated between the two pulses can therefore be detected directly in the reflected spectrum as a fringe shift. This technique allows to achieve very accurate measurements of the phase with an uncertainty of  $\pm 0.01$  radian, with a time resolution of the order of the duration of the probe pulse, and a spatial resolution along the focal diameter of  $\approx 3\text{-}\mu\text{m}$  [55]. Recent applications of phase measurement techniques involve direct observation of the ponderomotive force exerted on a plasma [65]. Figure 3 shows the phase shift of a S-polarized probe beam when two laser pulses (laser intensities of  $10^{15}$  and  $5 \times 10^{17}$  W/cm<sup>2</sup>) separated by 6-ps, the prepulse and the main pulse, are interacting with the target. Only the region corresponding to the center of the main pulse focal spot is shown. We clearly see that the interaction with the main pulse almost stops the plasma expansion. Ponderomotive force effects on plasmas have been used to increase the electron density in spectroscopic studies [66].

## 4 Ultrafast X-ray spectroscopy and X-ray sources

Once the low-absorption problem of ultrafast laser interaction has been solved, laser-plasmas have a number of characteristics [30, 67] that make them valuable as x-ray sources in time-resolved x-ray measurements: i) a

wide range of pulse durations from a few hundred femtoseconds to tens of picoseconds [68,69], ii) very bright x-ray sources can be generated with source sizes as small as a few microns, and iii) laser-plasma x-ray sources can be accurately synchronized with other events that can be driven, triggered or stimulated by the same laser light. Thermal x-ray emission from laser-produced plasmas in the subpicosecond regime occurs with pulse durations of the order of a few picoseconds [70–72], measured by a streak camera. Conversion efficiencies (i.e. the ratio of x-ray energy to laser energy) for radiation above one keV are of the order of  $10^{-5}$  in a single line, but conversions efficiencies around 200-eV are higher, about 0.1% for a 20% bandwidth [73].

Aluminum and silicon have been used as benchmark materials to spectroscopically study ultrafast plasmas. The conversion efficiency into narrow spectral lines and the duration of Al and Si thermal lines have been studied for a variety of experimental situations.

### Helium-like lines and satellites

Primarily, He-like ion and satellite emissions from lower-charge state ions have been studied extensively [37, 74–76]. H-like ions have been seldom seen in experiments because their emergence temperature is much higher at the laser intensities considered here. Stark broadening of the spectral lines and the strong influence of satellite lines originating from doubly-excited levels are the main results of these studies. Figure 4 shows the striking difference between short pulse (Fig.4a) and long pulse (Fig.4b) laser irradiation of a silicon target around the He-like resonance line and its Li-like and Be-like di-

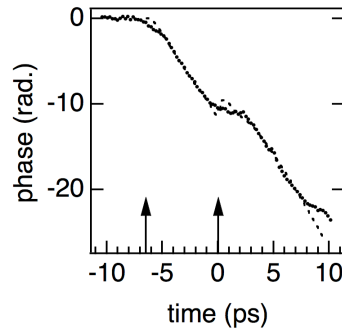


**Fig. 3.** Phase shift of S-polarized probe beam as a function of time following the interaction of a pure carbon target with a 400-fs duration laser pulse and prepulse (arrows). Experiment (dots) and FILM-fs simulations (solid line), see Sect.5, are compared for a prepulse delay of 6-ps. The peak of the main pulse is at time zero.

electronic satellites. Time duration of these kilovolt emissions have been studied with a sub-ps resolution streak camera [77,78], and conversion efficiencies have been determined for more energetic x-rays [79]. Spectroscopy of ultrafast plasmas has been performed with contrast-clean laser pulses obtained through frequency doubling [80,81] and tamped Al-tracer layer-targets [82]. Isochoric heating of solid aluminum at temperatures around 300-eV has been achieved. This corresponds to a pressure or energy density of  $\approx 0.4$ -Gbar in the heated dense aluminum. Free standing foils, 25-nm thin, have also been used to reach very high electron densities in contrast-clean experiments [83,84]. The small foil thickness in these experiments minimized thermal gradients in the longitudinal direction and allowed a simple physical interpretation of the spectral data.

### $K\alpha$ lines

It is well known [85] that ultra-intense laser pulse interaction with solid targets produce copious amounts of hot electrons. Collective absorption mechanisms transfer part of the laser energy into hot electrons which are accelerated to multi-kilovolt energies and penetrate into the “cold” solid behind the plasma where they generate x-rays via K-shell ionization and bremsstrahlung [18]. Resonance absorption is one of these collective mechanism that explains the sensitivity of hot electron conversion efficiency to laser polarization. Indeed, the conversion efficiency from laser light into K-shell line radiation in P-polarization is 100-times higher than the one measured in S-polarization. Suprathermal electrons produced by non-collisional absorption mechanisms have proved to be a convenient way of generating x-rays in the photon energy range above one keV [86]. In the 1- to 10-keV energy range, efficient

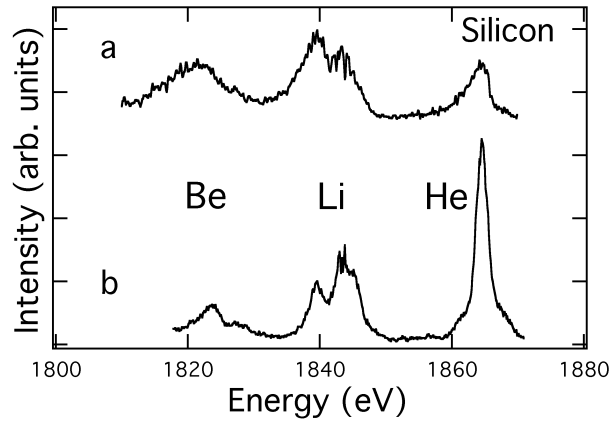


**Fig. 4.** Experimental Silicon spectrum associated to the Be-, Li-, and He-like ions, (a) short-pulse (0.12 – ps), (b) long-pulse (2.5 – ps).

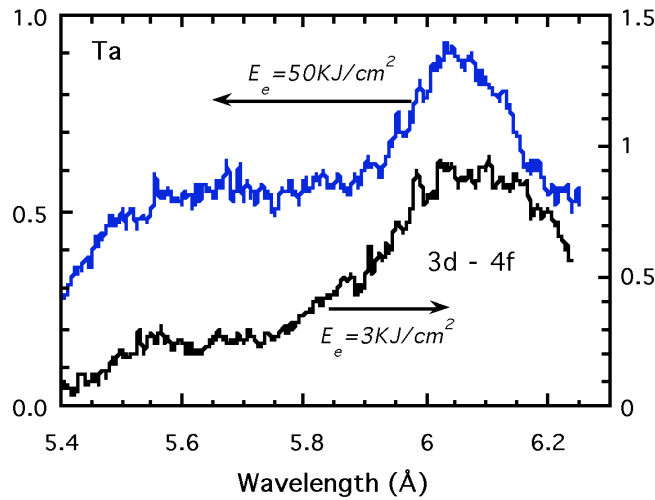


**Fig. 5.** Time-integrated spectra of the Ta 3d-4f transitions obtained for two different values of the hot electron energy density on target. Laser pulse is 400-fs long and intensity is  $5 \times 10^{18}$  W/cm<sup>2</sup>. Adapted from Ref. [94].

production of  $K_\alpha$  radiation in aluminum, calcium, and iron has been demonstrated. The x-ray throughput was controlled by varying the energy contrast ratio between the main ultrashort pulse and its nanosecond pedestal. The main characteristics of this type of source are a source diameter of about 10- $\mu$ m, repetition rate is 10-Hz and a total number of photons per shot of about  $3 \times 10^8$  to  $10^{10}$ , depending on laser intensities.  $K\alpha$  lines produced from ultrafast plasmas have been shown to be of a time duration similar to the laser pulse [87–89]. Supra-thermal electrons have also been used to investigate isochoric heating of solid matter. Temperatures of 500-eV and electron densities up to  $5 \times 10^{23}$  cm<sup>-3</sup> have been found. The heated depth is consistent with the range of 20-keV electrons, and the energy deposited in the heated layer was estimated to be a significant fraction (20 to 25%) of the incident laser energy [90].

### Broadband sources

Thermal emission from ultrafast plasmas is composed of discrete lines or very narrow bands of lines when targets of low atomic number  $Z$  are used. The effect of an increase of  $Z$  on the emission is that it changes the character of the thermal radiation from line to bands. In order to realize absorption spectroscopy one needs a backlight flash (multi-keV range) that is

quasi continuous in some region of interest. M-shell emission spectra, obtained with ultrafast lasers interacting with high- $Z$  material, have been measured recently [91, 92]. These spectra emitted by dense plasmas display broadband emissions related to Unresolved Transitions Arrays [93]. In Fig. 5 is shown broadband emission spectra of the 3d-4f transitions obtained for two different values of the energy contained in the hot electrons (equivalent to the laser intensity) when thick Ta targets are irradiated at  $5 \times 10^{18}$  W/cm<sup>2</sup> with 400-fs pulses. The observed ionization states seem to be slightly higher in presence of hot electrons (mostly Ga-like), compared to the result obtained with less hot electrons (mostly As-like) [94].

Laser-produced x-ray plasma sources can be distinguished by their high *peak* brightness. Increasing the laser repetition rate to boost their *average* brightness is not always practical [95,96]. Conventional laser-produced plasma targets produce debris which may destroy or coat sensitive x-ray components such as multilayer optics, Bragg crystals, or even the sample under study. The interaction of small rare gas clusters with short pulse high intensity lasers may be applied, in the future, to the production of short pulse x-rays without the complications of laser solid-target interaction [97].

### Harmonic generation on solids

High-harmonic generation with ultrashort laser sources has recently attracted great interest [98] as a convenient technique for the production of coherent EUV and XUV radiation. Until now, most high-harmonic-generation processes were studied in inert-gas and cluster targets [99]. High-harmonic generation from an overdense plasma surface operates at higher intensities [100]. The generation of harmonics from a ponderomotively driven oscillating plasma surface was studied theoretically by Lichters et al. [101] who used fully relativistic one-dimensional particle-in-cell simulations. Recent experiments show the importance of the laser intensity contrast ratio on harmonic generation [102,103]. A plasma mirror was designed and used to obtain 60-fs 10-TW laser pulses with a temporal contrast of  $10^8$  on a nanosecond time scale and  $10^6$  on a picosecond time scale. With these high-contrast pulses high harmonics were generated by nonlinear reflection on a plasma with a steep electronic density gradient. Well-collimated harmonics up to 20th order were observed for a laser intensity of  $3 \times 10^{17}$  W/cm<sup>2</sup>, whereas no harmonics are obtained without the plasma mirror [102]. Harmonics from the rear side of laser-irradiated thin foils are useful to probe plasmas. The highest harmonic generated in this way is near the plasma frequency of the dense foil. Above this frequency a cut off occurs, which is observed in experiments [104], and is of interest for diagnostics to determine the maximum density in the foil during the interaction.

## 5 Ultrafast plasma modeling

The various hydrodynamics codes which have been developed for laser-induced fusion [105] have all been rapidly adapted to treat the case of ultrashort pulse interaction. Different flavors of hydrocodes like FILM-fs [106], MULTI-fs [107] and UBC [108] are now available. The set of fluid equations that all these codes solve is:

$$\begin{aligned} \frac{\partial \rho}{\partial t} + \rho^2 \frac{\partial u}{\partial m} &= 0 \\ \frac{\partial u}{\partial t} + \frac{\partial(p_e + p_i)}{\partial m} &= 0 \\ \frac{\partial \epsilon_e}{\partial t} + p_e \frac{\partial u}{\partial m} &= -\frac{\partial S_e}{\partial m} - \sum_k \frac{\partial S_k}{\partial m} + \frac{\partial S_L}{\partial m} - \gamma(T_e - T_i) \\ \frac{\partial \epsilon_i}{\partial t} + p_i \frac{\partial u}{\partial m} &= \gamma(T_e - T_i) \end{aligned}$$

The system is closed by the equation of state (EOS) of the target material which relates the electron  $\epsilon_e$ ,  $p_e$  and ion  $\epsilon_i$ ,  $p_i$  energies and pressures to the density  $\rho$  and temperatures  $T_e$  and  $T_i$ .  $S_k$  is the radiative flow of photon group  $k$  with energies  $h\nu_k \leq h\nu \leq h\nu_{k+1}$ .  $S_e$  is the electron heat flow.  $S_L$  is the energy deposited by the laser. In the ultrashort pulse regime where energy is impinging on a steep density gradient,  $S_L$  is calculated by self-consistent solution of the Helmholtz equations using the Drude approximation to the dielectric constant. FILM-fs [106] incorporates the effects of the

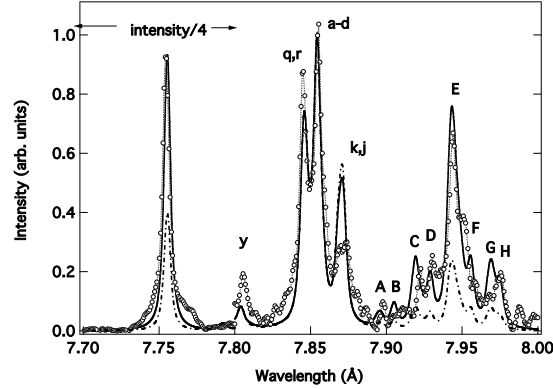


**Fig. 6.** Al spectrum of a 200-nm thin film irradiated at  $2 \times 10^{16}$  W/cm<sup>2</sup> compared to the result of time-dependent atomic physics and hydrodynamic calculations at  $10^{16}$  W/cm<sup>2</sup> (full) and  $3 \times 10^{16}$  W/cm<sup>2</sup> (chain). Heights are normalized to the experimental (a-d) peaks (following the notation of Gabriel [109]). The intensity of the He-like resonance line below 0.78-nm has been divided by four.

ponderomotive pressure (see above). These codes have not been developed to treat the relativistic regime  $I \geq 10^{18}$  W/cm<sup>2</sup>. Within the framework of the approximations made, such as the Drude model for electron conduction, there are a few adjustable parameters (within a restricted range governed by comparison to various experiments) to match the isochoric solid/warm plasma transition. These parameters are: the momentum transfer collision frequency which enters the dielectric constant formula, the electron-ion collision frequency for energy transfer entering the parameter  $\gamma$  in the hydrodynamic equations above, and the correct expressions of the electron and thermal conductivities.

LTE is seldom found in short pulse laser-produced plasmas because of time-dependent effects and steep spatial gradients. To simulate plasma line and continuum emissions, one has to rely on collisional-radiative models, such as TRANSPEC as a postprocessor [110]. In this type of code, one solves the full master equations for the ion level populations  $\{N\}$ :

$$\frac{d\{N\}}{dt} = \{A\}\{N\}$$

where  $\{A\}$  is the matrix of collisional and radiative excitation and de-excitation rate constants. Rates can be calculated in various ways, from detailed term accounting to the formalism of super-configuration arrays [111]. Experimental results and numerical simulations of K-shell emission from Be-like, Li-like and He-like ions from a 100-fs laser-produced aluminium plasma at intensities in excess of  $10^{16}$  Wcm<sup>-2</sup> have been obtained [75] that show (see Fig.6) that time-dependent modelling explains the much shorter than the laser pulse X-ray pulse duration of the Be-like and Li-like emissions [75].

## 6 Applications of ultrafast plasmas at low pulse energies

Absorption of ultra-short low-energy laser pulses takes place on a timescale much shorter than energy transfer of excited electrons to the lattice atoms (typically a few ps). The result is the creation of a highly ionized surface layer (plasma) at near solid density. Surface melting can virtually be eliminated along with plasma shielding, which takes place in typical nanosecond laser ablation [112]. Hence, femtosecond laser ablation can yield precise materials processing resulting from efficient energy deposition while simultaneously minimizing heat conduction and thermal damage to surrounding material. Focussed intensities  $I > 10^{13}$  W/cm<sup>2</sup> are easily obtained with micro-joule pulses and the processing of, for example, normally transparent dielectrics can be achieved through multi-photon absorption [113]. Metals can be ablated quite easily [114] and the absence of a heat affected zone (HAZ), like in ordinary ns-pulse material processing, makes femtosecond pulse micro-machining a fast developing technology. For the foreseeable future, femtosecond-based machining will be restricted mainly to applications that cannot be addressed with

other machining technologies [115, 116]. One such application is glass micro-machining, a much more subtle endeavor than machining of metals [112]. In summary, the hydrodynamics of material ejection into vacuum have been modeled to consider particle formation following energetic femtosecond laser ablation. The ejected material is quenched from 1 to 3 orders of magnitude more rapidly than is material on the bulk surface and therefore stands the best chance of trapping potentially unique material states associated with rapid quenching of an extreme material state. The mean particle diameter is estimated to range from 1- to 10-nm, and it should be possible to exercise some control over nanoparticle size by varying the laser fluence. Experimental determination of both nanoparticle size and associated electronic and structural properties remains an important goal [117].

## 7 Conclusions

Many fundamental processes in physics, materials science, chemistry, and biology occur on the ultrafast (picosecond or subpicosecond) time scale. Some of these processes can be initiated by transient optical excitation, and followed in their time evolution by ultrafast infrared, visible and ultraviolet spectroscopy. Pump-probe optical techniques are sensitive to electronic excitations, whereas extension to the sub-nanometer wavelength range should make possible the direct monitoring of atomic positions. Ultrafast laser-based plasma studies will play a pivotal role in the development of experimental dense plasma physics in the coming years. Ultrafast plasmas will also have important applications in material processing, thin film growth using ultrafast pulsed-laser deposition, and ultrashort pulse x-ray sources. Moreover, in the future, femtosecond x-ray pulses will have tremendous applications in broad areas of science, including condensed matter physics, chemistry, biology, and engineering because the ability to time-resolve atomic motions by x-ray diffraction (XRD) could open entirely new fields of scientific research [118]. The potentially most rewarding, but also most demanding application of femtosecond XRD will be the characterization of ultrafast structural processes in complex biological molecules.

## Acknowledgments

It is a pleasure to acknowledge the strong support of my colleagues Jean-Paul Geindre, Patrick Audebert, Claude Chenais-Popovics from Laboratoire d'Utilisation des Lasers Intenses, and Antoine Rousse from Laboratoire d'Optique Appliquée.

## References

1. P. Maine, D. Strickland, M. Pessot, J. Squier, P. Bado, G. Mourou, and D. Harter, *Chirped Pulse Amplification: Present and Future in Ultrafast Phenomena VI*, ed by T. Yajima, K. Yoshihara, C. B. Harris, and S. Shionoya (Springer-Verlag, New York, 1988), p. 205, and references therein.
2. G.A. Mourou, C.P. Barty, and M.D. Perry, *Physics Today*, January 98, 22 (1998).
3. D. Umstadter, *Phys. Plasmas* **8**, 1774 (2001).
4. V. Malka *et al.*, *Science* **298**, 1596 (2002).
5. M. Roth *et al.*, *Phys. Rev. STAB* **5**, 061031 (2002) and references therein.
6. S. P. D. Mangles *et al.*, *Nature* **431**, 535 (2004); C. G. R. Geddes *et al.*, *ibid.* **535** (2004); J. Faure *et al.*, *ibid.* **541** (2004).
7. S. V. Bulanov, T. Zh. Esirkepov, V. S. Khoroshkov, A. V. Kuznetsov and F. Pegoraro, *Physics Letters A* **299**, 247 (2002).
8. T. E. Cowan *et al.*, *Phys. Rev. Lett.* **92**, 204801 (2004).
9. M. Tabak, *Physics of Plasmas* **12**, 057305 (2005).
10. C. Rose-Petruck, R. Jimenez, T. Guo, A. Cavalleri, C.W. Siders, F. Ràski, J.A. Squier, B.C. Walker, K. Wilson and C.P.J. Barty, *Nature* **398**, 310 (1999).
11. J.C. Gauthier, *Dense Ultrafast Plasmas*, in *Atoms, Solids, and Plasmas in Super-Intense Fields*, ed D. Batani *et al.* (Kluwer Academic/Plenum Publishers, 2001) pp. 193-231.
12. X. Liu, D. Du, and G. Mourou, *IEEE J. Quantum Electron.* **33**, 1706 (1997).
13. E. G. Gamaly, A. V. Rode, and B. Luther-Davies, *J. Appl. Phys.* **85**, 4213 (1999).
14. A. Rousse, P. Audebert, J. P. Geindre, F. Fallières, J.-C. Gauthier, A. Mysyrowicz, G. Grillon, and A. Antonetti, *Phys. Rev. E* **50**, 2200 (1994).
15. W.L. Kruer, *The Physics of Laser Plasma Interactions*, (Addison-Wesley, Redwood-City, 1988).
16. E.M. Campbell, *Phys. Fluids B* **4**, 3781 (1992).
17. J.-C. Gauthier, *Short Pulse Laser Interaction With Solid Targets*, in *Laser Interaction with Matter*, ed S. Rose, (Institute of Physics Publishing, Bristol, 1995).
18. P. Gibbon and E. Förster, *Plasma Phys. Control. Fusion* **38**, 769 (1996).
19. J.-C. Kieffer, P. Audebert, M. Chaker, J.-P. Matte, H. Pépin, T.W. Johnston, P. Maine, D. Meyerhoffer, J. Delettrez, D. Strickland, P. Bado, and G. Mourou, *Phys. Rev. Lett.* **62**, 760 (1989).
20. H.M. Milchberg and R.R. Freeman, *J.O.S.A. B* **6**, 1351 (1989).
21. R. Fedosejevs, R. Ottmann, R. Sigel, G. Kuhnle, S. Szatmari, and F.P. Schäfer, *Phys. Rev. Lett.* **64**, 1250 (1990).
22. D.F. Price, R.M. More, R.S. Walling, G. Guethlein, R.L. Shepherd, R.E. Stewart, and W.E. White, *Phys. Rev. Lett.* **75**, 252 (1995).
23. F. Brunel, *Phys. Rev. Lett.* **59**, 152 (1987).
24. M.K. Grimes, Y.-S. Lee, A.R. Rundquist and M.C. Downer, *Phys. Rev. Lett.* **82**, 4010 (1999).
25. W. Rozmus and V.T. Tikhonchuk, *Phys. Rev. A* **42**, 7401 (1990); *ibid.* **46**, 7810 (1992)
26. A.A. Andreev, K.Yu. Platonov, and J.-C. Gauthier, *Phys. Rev. E* **58**, 2424 (1998).

27. M.M. Murnane, H.C. Kaypten, and R.W. Falcone, Phys. Rev. Lett. **62**, 155 (1989).
28. P. Audebert, J.-P. Geindre, J.-C. Gauthier, J.-P. Chambaret, A. Mysyrowicz, and A. Antonetti, Europhysics Letters **19**, 189 (1992).
29. S. Bastiani, A. Rousse, J.-P. Geindre, P. Audebert, C. Quiox, G. Hamoniaux, A. Antonetti, and J.-C. Gauthier, Phys. Rev. E **56**, 7179 (1997).
30. J.F. Pelletier, M. Chaker, and J.-C. Kieffer, J. Appl. Phys. **81**, 5980 (1997).
31. H. Nakano, T. Nishikawa, H. Ahn, and N. Uesugi, Appl. Phys. Lett. **69**, 2992 (1996).
32. M.M. Murnane, H.C. Kapteyn, S.P. Gordon, J. Bokor, E.N. Glytsis, and R.W. Falcone, Appl. Phys. Lett. **62**, 1068 (1993).
33. J.-C. Gauthier, S. Bastiani, P. Audebert, J.-P. Geindre, K. Neuman, T. Donnelly, M. Hoffer, R.W. Falcone, R. Shepherd, D. Price, et B. White, SPIE Proceedings **2523**, 242 (1995).
34. Tadashi Nishikawa, Hidetoshi Nakano, Naoshi Uesugi, Masashi Nakao, and Hideki Masuda, Appl. Phys. Lett. **75**, 4079 (1999); *ibid.* **70**, 1653 (1997).
35. G. Kulcsár, D. AlMawlawi, F.W. Budnik, P.R. Herman, M. Moskovits, L. Zhao, and R.S. Marjoribanks, Phys. Rev. Lett. **84**, 5149 (2000).
36. J.-C. Gauthier, S. Bastiani, P. Audebert, J.P. Geindre, K. Neuman, T. Donnelly, M. Hoffer, R.W. Falcone, R. Sheperd, D. Price and B. White, Proc. SPIE **2523**, 242 (1995).
37. R.C. Mancini, P. Audebert, J.-P. Geindre, A. Rousse, F. Fallis, J.-C. Gauthier, A Mysyrowicz, J.-P. Chambaret, and A. Antonetti, J. Phys. B: Atom. Optical Mol. Phys. **27**, 1671 (1994).
38. R. Benattar, J.P. Geindre, P. Audebert, J.-C.Gauthier, J.P. Chambaret, A. Mysyrowicz and A. Antonetti, Optics Commun. **88**, 376 (1992).
39. H.M. Michberg and R.R. Freeman, Phys. Rev. A **41**, 2211 (1990).
40. R. Sauerbrey, J. Fure, S.P. Le Blanc, B. van Wonterghem, U. Teubner and F.P. Schäfer, Phys. Plasmas **1**, 1635 (1994).
41. S.P. Le Blanc, R. Sauerbrey, J. Opt. Soc. Am. B **13**, 72 (1996).
42. Y.M. Li and R. Fedosejevs, Phys. Rev. E **54**, 2166 (1996).
43. W.M. Wood, C.W. Siders, and M.C. Downer, Phys.Rev. Lett. **67**, 3523 (1991).
44. C.W. Siders, N.C. Turner III, M.C. Downer, A. Babine, A. Stepanov, and A.M. Sergeev, J. Opt. Soc. Am. B **13**, 330 (1996).
45. K.Y. Kim *et al.* , Phys. Rev. A **71**, 011201 (2005).
46. T. Dewandre, J.R. Albritton, and E.A. Williams, Phys. Fluids **24**, 528 (1981).
47. O.L. Landen and W.E. Alley, Phys. Rev. A **48**, 5089 (1992).
48. X. Liu and D. Umstadter, Phys. Rev. Lett. **69**, 1935 (1992).
49. O.L. Landen, D.G. Stearns and E.M. Campbell, Phys. Rev. Lett. **63**, 1475 (1989).
50. Suipta Bera, A.J. Sabbah, C.G. Durfee, and J.A. Squier, Optics Letters **30**, 373 (2005).
51. J.-P. Geindre *et al.* , Optics Letters**19**, 1997 (1994).
52. N. Scherer *et al.* , J. Chem. Phys. **95**, 1487 (1991).
53. P. Audebert *et al.* , Phys. Rev. Lett. **73**, 1990 (1994).
54. F. Quéré, S. Guizard, and P. Martin, Europhysics Letters **56**, 138 (2001).
55. J.-R. Marquès *et al.* , Phys. Rev. Lett. **76**, 3566 (1996).
56. R. Evans *et al.* , Phys. Rev. Lett. **77**, 3359 (1996).
57. K.T. Gahagan, D.S. Moore, D.J. Fink, R.L. Rabie, and S.J. Bulow, Phys. Rev. Lett. **85**, 3205 (2000).

58. D.J. Fink *et al.*, Phys. Rev. B **64**, 115114 (2001).
59. P. Blanc *et al.*, J.O.S.A. B**13**, 118 (1996).
60. C. Quoix *et al.*, Eur. Phys. J. AP **5**, 163 (1999).
61. C. Quoix *et al.*, J.Q.R.S.T. **65**, 455 (2000).
62. A. Benuzzi-Mounaix *et al.*, Phys. Rev. E**60**, R2488 (1999).
63. S. Rebibo *et al.*, Laser and Particle Beams **19**, 67 (2001).
64. D. Descamps *et al.*, Optics Letters **25**, 135 (2000).
65. P. Audebert, J.-P. Geindre, S. Rebibo, et J.-C. Gauthier, Phys. Rev. E **64**, 056412 (2001).
66. O. Peyrusse, M. Busquet, J.-C. Kieffer, Z. Jiang, and C.Y. Côté, Phys. Rev. Lett. **75**, 3862 (1995).
67. C.Y. Côté, J.C. Kieffer, and O. Peyrusse, Phys. Rev. E **56**, 992 (1997).
68. I.C. Turcu and J.B. Dance, *X-Rays From Laser Plasmas*, (John Wiley and Sons, Chichester, 1999).
69. See several contributions in *New Ultrafast X-Ray Sources and Applications*, ed J.-C. Gauthier, C. R. Acad. Sci. Paris, Séries IV **1**, (Elsevier, Paris, 2000).
70. J. Workman A. Maksimchuk, X. Liu, U. Ellenberger, J.S. Coe, C.Y. Chien, and D. Umstadter, Phys. Rev. Lett. **75**, 2324 (1995).
71. J.F. Pelletier, M. Chaker, and J.C. Kieffer, Optics Letters **21**, 1040 (1996).
72. J. Workman, A. Maksimchuk, X. Liu, U. Ellenberger, J.S. Coe, X.-Y. Chien, and D. Umstadter, J.O.S.A. **13**, 125 (1996).
73. D. Alterbernd, U. Teubner, P. Gibbon, E. Förster, P. Audebert, J.P. Geindre, J.C. Gauthier, G. Grillon, and A. Antonetti, J. Phys. B: Atom. Mol. Opt. Phys. **30**, 3969 (1997).
74. G.A. Kyrala, R.D. Fulton, E.K.Wahlin, L.A.Jones, G.J? Schappert, and J.A. Cobble, Appl. Phys. Lett. **60**, 2195 (1992).
75. P. Audebert, J.-P. Geindre, A. Rousse, F. Fallis, J.-C. Gauthier, A Mysyrowicz, G. Grillon, and A. Antonetti, J. Phys. B: Atom. Optical Mol. Phys. **27**, 3303 (1994).
76. R.C. Mancini, A.S. Shlyaptseva, P. Audebert, J.-P. Geindre, S. Bastiani, J.-C. Gauthier, G. Grillon, A. Mysyrowicz, et A. Antonetti, Phys. Rev. E **54**, 4147 (1996).
77. Z. Jiang, J.-C. Kieffer, J.P. Matte, M. Chaker, O. Peyrusse, D. Gilles, G. Korn, A. Maksimchuk, S. Coe, and G. Mourou, Phys. Plasmas **2**, 1702 (1995).
78. C.Y. Côté, J.-C. Kieffer, Z. Jiang, A. Ikhlef, and H. Pépin, J. Phys. B: At. Mol. Opt. Phys. **31**, L883 (1998).
79. J. Yu, Z. Jiang, J.-C. Kieffer, and A. Krol, Phys. Plasmas **6**, 1318 (1999).
80. K. Eidmann, A. Saemann, U. Andiel, I. E. Golovkin, R. C. Mancini, E. Anderson, and E. Förster, J. Quant. Spectr. Rad. Transfer **65**, 173 (2000).
81. U. Andiel, K. Eidmann, K. Witte, I. Uschmann, and E. Förster, Appl. Phys. Lett. **80**, 198 (2002).
82. A. Saemann, K. Eidmann, I.E. Golovkin, R.C. Mancini, E. Anderson, E. Förster, and K. Witte, Phys. Rev. Lett. **82**, 4843 (1999).
83. P. Audebert, R. Shepherd, K. B. Fournier, O. Peyrusse, D. Price, R. W. Lee, P. Springer, J.-C. Gauthier, and L. Klein, Phys. Rev. E **66**, 066412 (2002).
84. P. Audebert, R. Shepherd, K. B. Fournier, O. Peyrusse, D. Price, R. Lee, P. Springer, J.-C. Gauthier, and L. Klein, Phys. Rev. Lett. **89**, 265001 (2002).
85. J. Lindl, Phys. Plasmas **2**, 3933 (1995).
86. A. Rousse, P. Audebert, J.-P. Geindre, F. Fallières, J.-C. Gauthier, A Mysyrowicz, G. Grillon, and A. Antonetti, Phys. Rev. **E50**, 2200 (1994).

87. Christian Rischel *et al.* , Nature, **390**, 497 (1997).
88. Ch. Reich, P. Gibbon, I. Uschmann, and E. Förster, Phys. Rev. Lett. **84**, 4846 (2000).
89. T. Feuer *et al.* , Phys. Rev. E **65**, 016412 (2001).
90. K. Eidmann *et al.* , in Atomic Processes in Plasmas, ed J. Cohen, S. Mazevet, and D. Kilcrease AIP Conference Proceedings **730**, pp. 81-93 (2004).
91. C. Chenais-Popovics *et al.* , in Laser-generated and other laboratory X-ray and EUV sources, optics, and applications, San Diego, CA, SPIE proceedings vol. 5196, 2003. Bellingham, WA: SPIE-International Society for Optical Engineering; 2004. p. 20512.
92. M. Busquet *et al.* , Phys. Rev. E **61**, 801 (2000).
93. J. Bauche and C. Bauche-Arnoult in Laser Interactions with Atoms, Solids and Plasmas, ed R. M. More (Plenum Press, New York, 1994).
94. J.C. Kieffer Ching Yuan Chien, Fabien Dorchies, Patrick Forget, Pascal Gallant, Zhiming Jiang and Henri Pépin in New Ultrafast X-Ray Sources and Applications, ed J.-C. Gauthier, C. R. Acad. Sci. Paris, Séries IV, **1**, (Elsevier, Paris, 2000), pp. 297-303.
95. Yan Jiang, T. Lee, and C.G. Rose-Petruck, J. Opt. Soc. Am. B **20**, 229 (2003).
96. A. Thoss *et al.* , J. Opt. Soc. Am. B **20**, 224 (2003).
97. F. Dorchies, T. Caillaud, F. Blasco, C. Bonté, H. Jouin, S. Micheau, B. Pons, and J. Stevefelt Phys. Rev. E **71**, 066410 (2005).
98. P. Balcou, R. Haroutunian, S. Sebban, *et al.* Appl. Phys. B **74**, 509 (2002).
99. T.D. Donnelly, T. Ditmire, K. Neuman, M.D. Perry, and R.W. Falcone, Phys. Rev. Letters **76**, 2472 (1996).
100. D. von der Linde, Appl. Phys. B **68**, 315 (1999).
101. R. Lichters, J. Meyer-ter-Vehn and A. Pukhov, Phys. Plasmas **3**, 3425 (1996).
102. P. Monot *et al.* , Optics Letters **29**, 893 (2004).
103. G. Doumy *et al.* , Physical Review E **69**, 026402 (2004).
104. U. Teubner *et al.* , Phys. Rev. Lett. **92**, 185001 (2004).
105. G.B. Zimmerman and W.L. Kruer, Comm. in Plasma Physics **11**, 51 (1975).
106. U. Teubner, P. Gibbon, E. Förster, F. Falliès, P. Audebert, J.-P. Geindre, and J.-C. Gauthier, Phys. Plasmas **3**, 2679 (1996).
107. K. Eidmann, J. Meyer-ter-Vehn, T. Schlegel, and S. Hüller, Phys. Rev. E **62**, 1202 (2000).
108. A. Forsman, A. Ng, G. Chiu, and R.M. More, Phys. Rev. E **58**, R1248 (1998).
109. A.H. Gabriel, Mon. Not. R. Astron. Soc. **160**, 99 (1972).
110. O. Peyrusse, Phys. Fluids **B4**, 2007 (1992); O. Peyrusse, J.Q.R.S.T. **51**, 281 (1994) .
111. O. Peyrusse, Nucl. Fusion **44** , S202 (2004).
112. E.G. Gamaly, A.V. Rode, B. Luther-Davies, and V.T. Tikhonchuk, Phys. Plasmas **9**, 949 (2002).
113. B.C. Stuart *et al.* , Phys. Rev. B **53**, 1749 (1996).
114. S. Nolte *et al.* , J. Opt. Soc. Am. B **14**, 2716 (1997).
115. X. Liu, D. Du, and G. Mourou, IEEE J. Quantum Electron. **33**, 1706 (1997).
116. P.P. Pronko, P.A. VanRompay, Z. Zhang, and J.A. Nees, Phys. Rev. Lett. **83**, 2596 (1999).
117. T.E. Glover, J. Opt. Soc. Am. B **20**, 131 (2003).
118. *Time-Resolved Diffraction*, ed by J.R. Helliwell and P.M. Rentzepis, (Oxford Science Publications, Clarendon, Oxford, 1997).